# The effects of hydroelectric dam construction on spatial-temporal changes of land use land cover in Bui National Park, Ghana

Godfred Bempah[1], Prince Boama[2] and Changhu Lu[3]

[1]College of Forestry, Nanjing Forestry University, China

[2]Resource Management Support Center, Forestry Commission, Ghana

[3]College of Biology and the Environment, Nanjing Forestry University, China

Corresponding author; [3]luchanghu@njfu.com.cn

Current address; Nanjing Forestry University, 159 Longpan Road, Nanjing, Jiangsu, China.

***Abstract***

Over the years, construction of hydroelectric dams has become part of the several initiatives to provide solution for the high demand of electricity in most countries. However, the construction of hydroelectric dams in forest reserves has become a matter of concern for policy and decision makers as well as biodiversity conservationists. Visibly among which is the potential to cause changes in land cover and subsequently affect fauna and flora composition. We analyzed the spatial-temporal changes of land use and cover in the Bui National Park using indices calculations of the landscape based on land cover maps obtained from Landsat satellite images at ten years intervals from 2000 - 2020. Land use indices calculation was done to assess the effects of pre-and post-dam construction. We found significant changes in land cover following the dam construction, notably, the built-up areas and water body, which recorded an increase of 315.64% and 4593.43% respectively due to the impoundment from 2010-2020, while the forest and

grassland decreased. The largest size of land conversion during the study was from open forest to grassland. Increased human activities such as illegal mining, indiscriminate tree fell, uncontrolled cattle grazing and charcoal production within the reserve as a result of the dam construction could likely compound the changes in land cover.

**Keywords:** landsat imagery; forest; grassland; conversion; settlement; impoundment

## Introduction

Land use relates to human use of an area of land, that is, whether for settlement, agriculture, forest, wildlife reserve etc. while land cover defines the ecological condition and physical appearance of the land surface (Geist & Lambin, 2002) e.g. grassland, forest, water, built-up/bare etc. on an area of land. Both land use and land cover (referred to as LULC) have a common causal agency and changes to the land, affecting both its use and cover. It exerts extensive environmental complications resulting from their combined effects on soil and water quality, biodiversity and microclimate (Schneider & Pontius, 2001). Changes in land use types often result in land cover changes; and human activities dominate the land use types, which therefore are the most influential causes of land cover changes (Turner & Meyer, 1991). Ghana has witnessed great changes in LULC within the past few decades as natural forests and savannah woodlands are converted to different forms such as agricultural lands, built up areas and open land (Antwi et al., 2014). Dakwa (2018) reported climate change to have accounted for the LULC at Mole National Park. At Bui National Park (BNP), the impoundment of the Black Volta River for hydroelectric development is envisaged to cause a major LULC change, involving about 21 percent of land mass of BNP that will be permanently inundated when it is fully impounded and this will lead to excessive effects of biodiversity loss, terrestrial and aquatic

ecosystems destruction, and most likely the influx of people into the area to influence land use changes (ERM, 2007; Tornyie & Kwapong, 2015).

Undoubtedly, human population expansion is a significant driving force for nearly all LULC changes (Serneels & Lambin, 2001) although other factors such as advancement in technology, wealth creation and changes in economic policies of governments may act in synergy with human population growth to influence LULC changes (Lambin et al., 2003) and this is now receiving considerable attention (Abdelali, 2018; Bird, 2012). One example is the construction of hydroelectric dams as part of the several initiatives to provide solution to the high demand by people for electricity in most countries (Kaunda et al., 2012). Globally, about 900,000 dams have produced about 16.3% of the world's total electricity supply (IEA, 2012) by modifying about 50% of large rivers (Nilsson et al., 2005).

In Ghana, there are three hydroelectric dams, namely, Akosombo (1,020 MW), Kpong (160MW) and Bui (404 MW), which are accessed by about 82.5% of the population for electricity (Hensengerth, 2011; International Hydropower Association, 2019). It appears the high demand for hydroelectricity is due to its cost effectiveness as well as impact on the environment compared to other power generating systems (Gaudard & Romerio, 2014) especially as green energy functioning in adaptation and mitigation of climate change (Bartle, 2002). However some negative environmental consequences come with the construction of hydroelectric dams (Beck et al., 2012; Kyei-Dompreh, 2012) including the flooding of large areas (Cunha & Ferreira, 2012; Woldemichael et al., 2012), which results in loss of biodiversity and riparian ecosystems (Ferreira, 2000; Cunha & Ferreira, 2012) and other related global environmental changes (Lambin et al., 2003) such as decreased area of forest land and increased area of agriculture land (Zhao et al., 2010). Yet others (Woldemichael et al., 2012) suggest a general increase in land

area used for non-agricultural purposes such as forest land, barren land and settlement and a reduced land area used for agricultural purposes.

Human activities around dams increase once the dams start operation (Woldemichael et al., 2012). In recent times, significant observable changes in LULC have occurred in BNP due to changes in land use patterns. In this regard, our main objective for this study is to assess the spatial-temporal dynamics of hydroelectric dam construction on the Bui natural ecosystems in order to review and implement environmental policies to manage, conserve and protect resources in the Bui National Park and its environs. Remote sensing and geographic information systems (GIS) provide powerful tools for change detection in LULC processes and their locations faster, at affordable rate and with improved precision (Herold et al., 2006).

In this study, we used post classification comparison method to classify satellite images with the Maximum Likelihood algorithm in a GIS environment to detect and evaluate LULC changes at BNP for three decade years, namely, 2000, 2010 and 2020. The use of post-classification comparison provides the most specific method and presents the advantage of detailing the nature of variations detected (Tendaupenyu et al., 2017).

## Method

### *Study area*

The Bui National Park (80 23' 13.2072" N, 20 22' 43.9788" W) covers an area of about 1,821 km² and it is located close to the Ghana-Cote D'Ivoire border (Figure 1). It is the third largest wildlife conservation area in Ghana. The Black Volta River bisects the park into two, with a portion lying in the north-western corner of the Banda district in the Bono Region and the other extending towards the southwestern part of the Bole district in the Savanna Region.

It was gazetted in 1971 to primarily provide protection for the drainage basin of the Black Volta River as well as to conserve biodiversity in the entire designated area.

The Park is renowned for its high biological richness. The vegetation of the area is mostly Guinea Savannah woodland with patches of Moist Semi-Deciduous Forest, harboring several animal species such as the hippopotamus (*Hippopotamus amphibious*), buffalo (*Syncerus caffer*), and roan antelope (*Hippotragus equinus*). The area experiences an average temperature of 24.5°C; relative humidity of about 75%; mean yearly rainfall ranges from 1140 mm to 1270 mm (Appiah et al., 2017). Altitude varies between 1,560 ~ 820 m a.s.l. The soil formation is characterized mostly by alluvial soils with few areas covered by red loams. The Bui hydroelectric dam is found at the southern end of the BNP. The dam is a gravity, roller-compacted concrete type with a height of a 110 m above foundation and creating a reservoir of 12,350 million $m^3$ with a total surface area of 440 $km^2$ (Habia, 2009; Obahoundje et al., 2018).

***Image Acquisition***

The land cover maps and matrixes were produced using remote-sensing and Geographic Information System (GIS) application. Landsat 7 Enhance Thematic Mapper Plus (ETM+) and Landsat 8 Operational Land Imager (OLI) images with little or no cloud cover for the years 2000, 2010 and 2020 were obtained from the United States Geological Survey (USGS) Global Visualization Viewer (GLOVIS) website (https://glovis.usgs.gov/). The percentage cloud cover information for each image was obtained from the metadata on the same website. Landsat image was used for this study because of its long coverage of the earth surface which spans from the 70s to date and its availability (open source and free).

All the shape files such as those of the community, road and the park had the same coordinate system, that is, Universal Transverse Mercator (UTM) Zone 30 North. This was to avoid geometric errors associated with working with data with different coordinate systems and ensure consistency and precision. All the satellite images were co-registered to ensure they were aligned with corresponding pixels representing the same objects.

***Image Preprocessing***

Data were prepared to compensate for systematic errors before analyses. Duggin and Robinov (1990) expect such errors to come from sensor spectral properties, atmospheric scattering, among others and to creep into the data acquisition process to reduce the quality of the remote sensor data. Since the errors could cause difficulties in comparing more than one images of the same scene, picked under different conditions, it was important to remove these effects. Therefore, (1) scan lines error associated with Landsat 7 caused by malfunctioning of the sensor were corrected by using the focal analysis tool in Erdas Imagine 2018 to fill in the gaps created by these scan lines. (2) Landsat tiles are made up of bands, each defined by the particular range of wavelength within which it captures radiation to produce image (Lillesand et al., 2015). The layer stack tool in Erdas Imagine 2018 was used to stack the bands for each tile to generate a composite image to obtain more spectral information from the composite image than analyzing the individual bands separately (Lillesand et al., 2015). (3) Haze has an additive effect to the overall image, resulting in higher digital number (DN) values, and as such, it is reducing the contrast (Lillesand et al., 2015). Its impact differs per band, highest in the blue range, lowest in the IR range (Lillesand et al., 2015). The “haze correction” tool in Erdas Imagine 2018 was used for this operation. This tool identifies the lowest DN value in each band then subtracts it from the remaining DN values for each band. This operation improves the contrast of the images. The composite images

generated from the layer stack operation were used as inputs for this operation. To improve the visualization of the images, image enhancement technique called histogram equalization was performed. This was done in Erdas Image 2018 using the "histogram equalize" tool. This operation further enhances the contrast and makes easy to detect subtle differences among earth surface features identified in the images. (4) The interest of this study was to analyze the land use changes within the study area and since the Landsat images extend beyond its boundary there was a need to extract areas that fell within it for further analysis. The "clip" tool under the data management toolbox in ArcGIS 10.5 was used to extract areas of the composite images (outputs from the haze correction) that fell within the study area.

***Image Classification***

Classification of image was carried out in two modes, unsupervised and supervised classification. This is performed to establish and earmark real world thematic classes to the image pixels (Lillesand et al., 2015).

***Unsupervised Classification***

In the unsupervised classification method, the computer software categorizes the pixels into common land use types using their spectral characteristics without any training data (Lillesand et al., 2015). In this study the isodata unsupervised classification algorithm in Erdas Imagine 2018 was used to classify each clipped image (output from the clip operation) into 30 – 40 classes. The classes were merged based on the spectral similarities to form 8 – 10 classes. The study area, community and road shape files were overlaid on the outputs to check the distribution of these classes within the study area and for easy navigation for field data collection. A map was produced from the 2020 classified image of the study area, which extended to the community,

and included the roads. This was used as preliminary map for field data collection, during which pixels picked from the unsupervised classification where traced on the field.

***Field Data Collection***

This was necessary to take coordinates of the various land cover types identified as training datasets from the supervised mode. The data collected were numbered serially and divided into two with one half (even numbers) used for training of the images and the other half (odd numbers) for ground truth accuracy assessment of the classified images. The data collected from the field included the coordinates of the points using GPS receiver, the land use description at that point. All the data were entered into a field sheet and later transferred into a Microsoft Excel Sheet. The field data were grouped according to the land cover types identified.

***Supervised Classification***

Here, the pixel categorization process is supervised by an analyst by identifying clearly, to the computer algorithm, numerical descriptors of the various land cover types existing in a location on the field (Lillesand et al., 2015). The classification was done in Erdas Imagine 2018, by using the polygon tool in training the pixels and introducing subclasses of land use types to reduce the margin of error. The maximum likelihood algorithm was then used in running the classification as it considers the cluster center and also its shape, size and orientation by calculating a statistical distance based on the mean values and covariance matrix of the clusters (Bakker et al., 2004). After the classification, the outputs were displayed in ArcGis 10.5 and the subclasses were together using the reclass tool. The reclassified maps were then filtered using the “majority filter” tool in ArcGIS 10.3.

### *Accuracy Assessment and Change Detection*

The field data were the reference data used to assess the accuracy of the classification and the confusion matrix and kappa statistics used to produce statistical outputs to check the quality of the classification results. Information on variations corresponding to trend, spatial distribution and extent of change can be obtained from change detection applications (Singh, 1989). The "matrix union" tool in Erdas Imagine 2018 was used to detect pixel by pixel changes to the final land cover maps. Thus it picked a pixel from the old land use map and compared it to the same pixel on the new land use map and so change matrix were generated from the change maps, which provided information on change detection in hectares of land cover or use.

The formula from Zhao et al. (2010) was adopted to determine amplitude of variation which expresses overall changes in the different land cover types:

$$Rd = ( Ua - Ub ) / Ua \times 100\% \quad \ldots\ldots\ldots\ldots\ldots\ldots\ldots\ldots\ldots\ldots \quad (1)$$

Where Rd is the calculated amplitude of variation, Ua and Ub refer to the areas of single type at the start and at the end of the various study periods respectively.

## Results

### *Land cover status*

In all, five land cover types were identified, namely; built-up, close forest, grassland, open forest, and water body (Table 1). A set of three different land cover maps covering the study area for the years 2000, 2010 and 2020 is shown in Figure 2. In 2020, open forest largely occupied the southeastern part of the study area, while grassland predominantly spread from the middle of the protected area towards the northern part with some few patches found in the southern part especially close to the lake banks (Figure 2). Majority of the water body is concentrated in the

southern to middle areas (Figure 2) resulting from the reservoir created due to the dam. Built-up area is largely found along the riverbanks and northeastern part of the study area (Figure 2) but few are also scattered within the southern and middle part of the study area (Figure 2).

In 2000, open forest occupied the largest portion of the total land area with 45.87% followed by grassland and close forest with 43.76% and 6.81% respectively (Figure 3a). In 2010 grassland occupied the largest portion with 63.45%, followed by open forest and close forest with 31.52% and 3.82% respectively (Figure 3b). In 2020, grassland occupied the largest percentage cover with 60.54%, followed by water body with 19.01% and open forest with 16.83% (Figure 3c).

***Land cover change***

Throughout the study period, we observed the highest area change in the water body, which increased by 4,593.43%, from 752.69 ha in 2010 to 35,326.39 ha in 2020 (Table 2). However, water body decreased slightly from 1,217.89 ha in 2000 to 752.65 ha in 2010, the period during which the dam was under construction. Close and open forest areas decreased from 12,647.01 ha and 85,243.78 ha in the year 2000 to 575.73 ha and 31,282.72 ha in 2020 respectively, representing 95.45% and 63.3% decreases respectively (Table 2). During the same period, grassland and built-up areas increased with the variation ratios reaching 38.32 % and 13.95 %, respectively (Table 2).

Noticeably, built-up areas decreased by 72.55% before the dam construction in the period of 2000-2010 but significantly increased by 315.08% after the construction of the dam in the period of 2010-2020 (Table 2). In general, from 2000 to 2020, the non-forest land increased greatly by 2852.89%, while forest land declined by 158.75% (Table 2).

### *Transfer area matrix of land cover types*

About 38.53% of the total land cover remained stable while about 61.47% was converted during the study period (Table 3). Transfer area of 52,444.72 ha from open forest to grassland marked the highest conversion over the study period (Table 4). Comparing the three decade years; 2000 and 2010, 2000 and 2020, and 2010 and 2020, the trend of conversion was almost consistent.

For example, conversion from open forest to grassland vis-a-viz other possible conversions involved the largest transfer area all the time, such as 43,910.05 ha, 52,444.72 ha and 26,899.64 ha, respectively (Table 4). Another major and much visible conversion was from grassland to water body from 2010 to 2020, involving transfer area of 17,526.41 ha and from open forest to water body with transfer area of 15,298.44 ha (Table 4). Conversion of all other land cover types to water body was basically due to inundation caused by the restricted water reservoir after the completion of the dam construction, though the construction itself caused a lot of damages and changes that facilitated conversion. Grassland and open forest were major converts to built-up area after the dam construction, with transfer areas reaching 4,937.69 ha and 1,018.67 ha respectively (Table 4).

### *Accuracy assessment*

The overall accuracy for 2000, 2010 and 2020 were 86.67%, 81.67% and 83.33% respectively (Table 5). We recorded the highest validation data for 2000, while that of 2010 were of least quality. The figures indicate that the land cover classification for the periods 2000, 2010 and 2020 were correctly classified. The calculated Kappa coefficients were 81%, 73.89%, and 77.32%, respectively, for 2000, 2010 and 2020 (Table 5), representing strong agreement.

## Discussion

There were significant changes in land cover of the Bui National Park (BNP) over the study period, from 2000 to 2020. The decrease in forest cover (close and open) at BNP is consistent with the national rate of deforestation occurring in Ghana (Antwi et al., 2014) and with the results of other studies (Zhao et al., 2010; Appiah et al., 2017) that found a decrease in forest cover after dam construction. Contrarily, Wiejaczka et al. (2017) found no significant changes in forest cover during pre-and post-dam construction.

Several factors may account for the deforestation rate in BNP including; (1) ineffective monitoring of contractors who were permitted to fell trees in the flood zones and therefore allowing indiscriminate felling of trees in the national park; (2) laxity in enforcing laws that protect national park most especially during and after construction of the dam; (3) lack of collaboration and cooperation among institutions responsible for managing the area and stakeholders, to team up to formulate integrated plans to secure the area during and after the project.

Post-dam (2010-2020) reduction in forest cover was more noticeable than pre-dam (2000-2010) reduction. Tree felling activities started from 2008 suggesting that between 2008 and 2010, tree felling activities were officially on going. It is then possible to explain that the deforestation that occurred before 2010 were largely due to preparation towards the construction of the dam. Tree felling activities were still carried out even after the completion of the dam, possibly resulting in the significant decrease in forest cover. Except for the trees found at the riverbanks, it is highly impossible to find a cluster of economic tree species in the study area. This explains the severity of the situation in terms of biodiversity conservation as well as climate change.

These migrants cut trees to build their houses and also as source of energy (firewood) for cooking. Trees were also cut to put up accommodation for resettled communities as well as for staff of the Bui National Park and Bui hydroelectric dam (Appiah et al., 2017).

Predominantly, the settlers are made of fisher folks who are found along the lake and riverbanks (Appiah et al., 2017). There is also significant number of illegal miners settled in the area, as well as cattle herdsmen and charcoal producers. Many small villages are scattered inside the reserve, and several others exist along the fringes. The huge number of people present in and outside the BNP carrying out several activities (Appiah et al., 2017) is linked to exploitation of forest resources on a daily basis (Sharma et al., 2019). These anthropogenic activities are escalating, affecting the reserve resources due to the continuous illegal entry of people into the reserve.

The water bodies increased significantly during the post-dam construction period, which can be attributed to the increase in the level of the reservoir created by the hydroelectric dam in the BNP, an observation that has been reported by other similar studies elsewhere (Obahoundje et al., 2018; Wiejaczka et al., 2017; Zhao et al., 2010).

The grassland decreased its cover from 2010-2020. Other researches (Chalise et al., 2019; Özüpekçe, 2019; Wiejaczka et al., 2017; Xu & Chi, 2019) have reported similar occurrence of post-dam grassland decline in protected areas. Illegal mining, uncontrolled cattle grazing and charcoal production could account for the decline of grassland during this period. Periodic movement of thousands of cattle within the reserve occurs and this leads to grass trampling and overgrazing.

This causes reduction in quality and quantity of forage as well as modifying vegetation and soil formation due to soil compaction (Obahoundje et al., 2018; Panthi et al., 2017; Sharma et al., 2019). In some cases, cattle herdsmen attempt to cause regeneration of fresh pasture by consciously setting fire to the vegetation resulting in uncontrolled destruction of vegetation (Sharma et al., 2019).

The changes in the built-up areas were significant during post-dam construction period, and consistent with reports of several studies (Zhao et al., 2010; Özüpekçe, 2019). The increase in built-up areas can be attributed to the emergency of illegal mining observed during field data collection. In nearly all cases of the reports as well as this study, gold mining is cited as the cause of increased sizes of the built-up areas and the incidence of illegal mining is attracting many young people to the area. A serious issue of encroachment lingers on, in the study area contributing to occurrence of built-up/bare lands.

## Conclusion

The main land cover structures that experienced greater changes are close forest, built-up areas and water body, more especially during the post-dam construction period. The changes involved conversion of one land cover type to another leading to transfer of sizeable cover from one type to another to cause a decrease or increase of any particular type involved. The post-dam changes also resulted in land use changes. Notable of this are the reduced size of the reserved forests of the national park, increased water covered surface and increased human settlements. The activities of the human settlements in particular are feared to compound the changes in land use. Therefore, a greater cooperation between the BNP and Bui Power Authority, which are the two institutions managing the area, is suggested, to ensure committed enforcement of protective laws and prevent further migration of people into the protected area.

**Acknowledgement**

We would like to thank the management and staff of Bui National Park for the assistance provided to us during the field data collection.

**Funding**

This research received no external funding

**Data Availability Statement**

The data presented in this study were obtained from the United States Geological Survey (USGS) Global Visualization Viewer (GLOVIS) at https://glovis.usgs.gov/

**References**

Abdelali, K. M, Taştan, Y., & Sönmez, A. Y. (2018). Investigation of Beyler dam lake water quality in terms of some physical and chemical parameters. *Marine Science and Technology Bulletin*. 7:21-27. https://doi.org/10.33714/masteb.399891

Antwi, E. K., Boakye-Danquah, J., Asabere, S. B., Yiran, G. A., Loh, S. K., Awere, K. G., ... & Owusu, A. B. (2014). Land use and landscape structural changes in the ecoregions of Ghana. *Journal of Disaster Research*, *9*(4), 452-467. https://doi.org/10.20965/jdr.2014.p0452

Appiah, D. O., Sarfo, M., Famieh, B., & Addai, H. (2017). Environmental and socioeconomic perturbations of a dam project on catchment communities, Ghana. *Global Environmental Health and Safety*, *1*, 1-9.

Bakker, W. H. et al (2004). Principles of Remote Sensing: An introductory textbook (3th Edition). The International Institute for Geo-Information Science and Earth Observation (ITC): Enschede, The Netherlands. https://webapps.itc.utwente.nl/librarywww/papers_2009/general/PrinciplesRemoteSensing.pdf

Bartle, A. (2002). Hydropower potential and development activities. Energy Policy. *Basin Man* 10: 73-92. https://doi.org/10.1016/S0301-4215(02)00084-8

Beck, M. W., Claassen, A. H., & Hundt, P. J. (2012). Environmental and livelihood impacts of dams: common lessons across development gradients that challenge sustainability. *International journal of river basin management*, *10*(1), 73-92. https://doi.org/10.1080/15715124.2012.656133

Bird, E. (2012). *The Socioeconomic Impact of Hydroelectric Dams on Developing Communities: A Case Study of the Chalillo Dam and the Communities of the Macal River Valley, Cayo District, Belize, Central America*, Environmental Studies Electronic Thesis Collection Paper 14: 115. https://scholarworks.uvm.edu/envstheses/14/

Chalise, D., Kumar, L., & Kristiansen, P. (2019). Land degradation by soil erosion in Nepal: a review. *Soil Systems*, *3*(1), 12. https://doi.org/10.3390/soilsystems3010012

Cunha, D. D. A., & Ferreira, L. V. (2012). Impacts of the Belo Monte hydroelectric dam construction on pioneer vegetation formations along the Xingu River, Pará State, Brazil. *Brazilian Journal of Botany*, *35*(2), 159-167. https://doi.org/10.1590/S0100-84042012000200005

Dakwa, K. B. (2018). Effects of Climate and Land Cover Changes on Habitat for Herbivores at Mole National Park, Ghana. *West African Journal of Applied Ecology*, *26*(2), 1-13.

https://www.ajol.info/index.php/wajae/article/view/182525

Duggin, M. J., & Robinov, C. J. (1990). Assumptions implicit in remote sensing data acquisition and analysis. *International Journal of Remote Sensing*, 11, 1669-1694. https://doi.org/10.1080/01431169008955124

ERM (Environmental Resources Management, 2007). Environmental and Social Management Plan (ESMP) for the Bui Hydroelectric Power Project. Prepared by Environmental resources Management, in association with SGS Environment for the Ministry of Energy/Bui Development Committee, Ghana, www.erm.com

Ferreira, L. V. (2000). Effects of flooding duration on species richness, floristic composition and forest structure in river margin habitat in Amazonian blackwater forests: implications for future design of protected areas. *Biodiversity and Conservation*, 9:1-14. https://link.springer.com/article/10.1023/A:1008989811637

Gaudard, L., & Romerio, F. (2014). Reprint of "The future of hydropower in Europe: Interconnecting climate, markets and policies". *Environmental Science & Policy*, 43, 5-14. https://doi.org/10.1016/j.envsci.2014.05.005

Geist, H. J., & Lambin, E. F. (2002). Proximate Causes and Underlying Driving Forces of Tropical Deforestation: Tropical forests are disappearing as the result of many pressures, both local and regional, acting in various combinations in different geographical locations. *BioScience*, *52*(2), 143-150 https://doi.org/10.1641/0006-3568(2002)052[0143:PCAUDF]2.0.CO;2

Habia, J. K. (2009). *The Bui dam impact on Ghana-China relations: transparency, accountability and development outcomes from China's sino hydro dam project in Ghana* (Doctoral dissertation, Massachusetts Institute of Technology).

https://core.ac.uk/download/pdf/4419663.pdf

Hensengerth, O. (2014). Interaction of Chinese institutions with host governments in dam construction: the Bui Dam in Ghana. In *Evolution of Dam Policies* (pp. 229-271). Springer, Berlin, Heidelberg. https://link.springer.com/chapter/10.1007/978-3-642-23403-3_8

Herold, M., Woodcock, C. E., Di Gregorio, A., Mayaux, P., Belward, A. S., Latham, J., & Schmullius, C. C. (2006). A joint initiative for harmonization and validation of land cover datasets. *IEEE Transactions on Geoscience and Remote Sensing*, *44*(7), 1719-1727. DOI: 10.1109/TGRS.2006.871219

IEA (2012), *Technology Roadmap - Hydropower*, IEA, Paris. https://www.iea.org/reports/technology-roadmap-hydropower

International Hydropower Association (2019). Ghana, Generation by hydropower https://www.hydropower.org/country-profiles/ghana

Kaunda, C. S., Kimambo, C. Z., & Nielsen, T. K. (2012). Hydropower in the context of sustainable energy supply: a review of technologies and challenges. *International Scholarly Research Notices*. https://doi.org/10.5402/2012/730631

Kyei-Dompreh, F. (2012). *Management of VRA Resettlement Towns: Case Study, West Kpong Resettlement Town* (Doctoral dissertation). Institute of Distance Learning Kwame Nkrumah University Science of Technology Kumasi Ghana. http://ir.knust.edu.gh/bitstream/123456789/4829/1/Kyei%20%E2%80%93Dompreh%20frederick.pdf

Lambin, E. F., Geist, H. J., & Lepers, E. (2003). Dynamics of land-use and land-cover change in tropical regions. *Annual review of environment and resources*, 28(1), 205-241.

https://doi.org/10.1146/annurev.energy.28.050302.105459

Lillesand, T., Kiefer, R. W., & Chipman, J. (2015). *Remote sensing and image interpretation*. John Wiley & Sons, Inc, Hoboken. https://books.google.com.gh/books

Nilsson, C., Reidy, C. A., Dynesius, M., & Revenga, C. (2005). Fragmentation and flow regulation of the world's large river systems. *Science*, 308:405–408. PMID: 15831757 https://doi.org/10.1126/science.1107887

Obahoundje, S., Diedhiou, A., Ofosu, E. A., Anquetin, S., François, B., Adounkpe, J., ... & Youan Ta, M. (2018). Assessment of spatio-temporal changes of land use and land cover over South-Western African basins and their relations with variations of discharges. *Hydrology*, *5*(4), 56. https://doi.org/10.3390/hydrology5040056

Özüpekçe, S. (2019). Investigation of Impact of Aslantaş Dam on Surrounding Environment Using Remote Sensing and GIS. *J Remote Sens GIS*, *8*(260), 2. https://doi.org/10.4172/2469-4134.1000260

Panthi, S., Khanal, G., Acharya, K. P., Aryal, A., & Srivathsa, A. (2017). Large anthropogenic impacts on a charismatic small carnivore: Insights from distribution surveys of red panda Ailurus fulgens in Nepal. *PLoS One*, *12*(7), e0180978. https://doi.org/10.1371/journal.pone.0180978

Schneider, L. C., & Pontius Jr, R. G. (2001). Modeling land-use change in the Ipswich watershed, Massachusetts, USA. *Agriculture, Ecosystems & Environment*, *85*(1-3), 83-94. https://doi.org/10.1016/S0167-8809(01)00189-X

Serneels, S., & Lambin, E. F. (2001). Proximate causes of land-use change in Narok District, Kenya: a spatial statistical model. *Agriculture, Ecosystems & Environment*, *85*(1-3), 65-81. https://doi.org/10.1016/S0167-8809(01)00188-8

Sharma, K., Robeson, S. M., Thapa, P., & Saikia, A. (2017). Land-use/land-cover change and forest fragmentation in the Jigme Dorji National Park, Bhutan. *Physical Geography*, *38*(1), 18-35. https://doi.org/10.1080/02723646.2016.1248212

Sharma, S., Bista, M., & Mingshi, L. (2019). Characterizing changes in land cover and forest fragmentation in Dhorpatan Hunting Reserve of Nepal from multi-temporal Landsat observations (1993-2018). *bioRxiv*, 846741. https://doi.org/10.1101/846741

Singh, A. (1989). Digital Change Detection Techniques using Remotely-Sensed Data. *International Journal of Remote Sensing*, 10 (6), 989-1003. https://doi.org/10.1080/01431168908903939

Stevens, K., Campbell, L., Urquhart, G., Kramer, D., & Qi, J. (2011). Examining complexities of forest cover change during armed conflict on Nicaragua's Atlantic Coast. *Biodiversity and Conservation*, *20*(12), 2597-2613. https://link.springer.com/article/10.1007/s10531-011-0093-1

Tendaupenyu, P., Magadza, C. H. D., & Murwira, A. (2017). Changes in landuse/landcover patterns and human population growth in the Lake Chivero catchment, Zimbabwe. *Geocarto International*, *32*(7), 797-811. https://doi.org/10.1080/10106049.2016.1178815

Tornyie, F., & Kwapong, P.K. (2015). Nesting ecology of stingless bees and potential threats to their survival within selected landscapes in the northern Volta region of Ghana. *African Journal of Ecology*, 53: 398-405. https://doi.org/10.1111/aje.12208

Turner, B., & Meyer, W. B. (1991). Land use and land cover in global environmental change: considerations for study. *International Social Science Journal*, *43*(130), 669-679. https://asu.pure.elsevier.com/en/publications/land-use-and-land-cover-in-global

Wiejaczka, Ł., Olędzki, J. R., Bucała-Hrabia, A., & Kijowska-Strugała, M. (2017). A spatial and temporal analysis of land use changes in two mountain valleys: with and without dam reservoir (Polish Carpathians). *Quaestiones Geographicae*, *36*(1), 129-137 https://doi.org/10.1515/quageo-2017-0010

Woldemichael, A. T., Hossain F., Pielke R., & Beltrán-Przekurat, A. (2012). Understanding the impact of dam-triggered land use/land cover change on the modification of extreme precipitation. *Water Resources Research*, 48 (9): 1–16. https://doi.org/10.1029/2011WR011684

Xu, F., & Chi, G. (2019). Spatiotemporal variations of land use intensity and its driving forces in China, 2000–2010. *Regional Environmental Change*, *19*(8), 2583-2596 https://doi.org/10.1007/s10113-019-01574-9

Zhao, Q., Liu, S., & Dong, S. (2010). Effect of dam construction on spatial-temporal change of land use: a case study of Manwan, Lancang River, Yunnan, China. *Procedia Environmental Sciences*, *2*, 852-858. https://doi.org/10.1016/j.proenv.2010.10.096

Table 1: Land cover Description

| Land cover | Description |
|---|---|
| Built-up | Building, cleared areas, mining sites, farms, bare land and rocky surfaces |
| Close forest | Dense woodland with trees canopy cover of more than 60% |
| Grassland | Shrubs, tree grass mosaic |
| Open forest | Open woodland with trees canopy cover between 15% - 59% |
| Water body | Rivers and Lake |

Table 2: Area and percentage changes of land cover in different year (ha, %).

| Land cover class | 2000 | | 2010 | | 2020 | | 2000-2010 | 2000-2020 | 2010-2020 |
|---|---|---|---|---|---|---|---|---|---|
| | Area (ha) | % | Area (ha) | % | Area (ha) | % | % | % | % |
| Close Forest | 1,2647.01 | 6.81 | 7,109.42 | 3.82 | 575.73 | 0.31 | -43.78 | -95.45 | -91.9 |
| Open Forest | 85,243.78 | 45.87 | 58,583.12 | 31.52 | 31,282.72 | 16.83 | -31.27 | -63.3 | -46.6 |
| Water | 1,217.89 | 0.65 | 752.69 | 0.41 | 35,326.39 | 19.01 | -38.2 | 2800.62 | 4593.43 |
| Grassland | 81,339.63 | 43.76 | 117,926.1 | 63.45 | 112,509.7 | 60.54 | 44.98 | 38.32 | -4.59 |
| Built-up | 5,404.75 | 2.91 | 1,481.69 | 0.8 | 6,158.48 | 3.31 | -72.58 | 13.95 | 315.64 |
| Total | 185,853.1 | 100 | 185,853.1 | 100 | 185,853.1 | 100 | | | |

Table 3: Percentage change to land area between decade years

| Period | Land area (%) | |
|---|---|---|
| | stable | conversion |
| 2000 - 2020 | 38.53 | 61.47 |
| 2000 - 2010 | 58.01 | 41.99 |
| 2010 - 2020 | 52.06 | 47.94 |

Table 4: The transfer area matrixes of land cover types from 2000 to 2010, 2000 to 2020, and 2010 to 2020 (ha).

| Year | | | | 2010 | | | |
|---|---|---|---|---|---|---|---|
| | Land cover type | Close Forest | Open Forest | Water | Grassland | Built-up | Total |
| | Close Forest | 3,123.5 | 6,552.53 | 54.4 | 2,888.1 | 28.48 | 12,647.01 |
| | Open Forest | 3,085.26 | 37,692.67 | 17.43 | 43,910.05 | 538.37 | 85,243.78 |
| 2000 | Water | 39.9 | 352.58 | 628.44 | 193.62 | 3.35 | 1,217.89 |
| | Grassland | 850.74 | 13,390.9 | 52.4 | 66,250.81 | 794.78 | 81,339.63 |
| | Built-up | 10.02 | 594.44 | 0.02 | 4,683.56 | 116.71 | 5,404.75 |
| | Total | 7,109.42 | 58,583.12 | 752.69 | 117,926.14 | 1,481.69 | 185,853.1 |

| | | | | 2020 | | | |
|---|---|---|---|---|---|---|---|
| | Land cover type | Close Forest | Open Forest | Water | Grassland | Built-up | Total |
| | Close Forest | 417.33 | 4,768.48 | 3,344.27 | 4,063.42 | 53.51 | 12,647.01 |
| | Open Forest | 149.07 | 17,108.39 | 13,493.37 | 52,444.72 | 2,048.23 | 85,243.78 |
| 2000 | Water | 5.15 | 45.39 | 1,108.39 | 57.51 | 1.45 | 1,217.89 |
| | Grassland | 4.17 | 8,865.29 | 16,721.28 | 52,332.98 | 3,415.91 | 81,339.63 |
| | Built-up | 0.01 | 495.17 | 659.08 | 3,611.11 | 639.38 | 5,404.75 |
| | Total | 575.73 | 31,282.72 | 35,326.39 | 112,509.74 | 6,158.48 | 185,853.1 |

| | | | | 2020 | | | |
|---|---|---|---|---|---|---|---|
| | Land cover type | Close Forest | Open Forest | Water | Grassland | Built-up | Total |
| | Close Forest | 271.4 | 3,205.34 | 1,684.26 | 1,925.78 | 22.64 | 7,109.42 |
| | Open Forest | 289.18 | 12,849.22 | 17,526.41 | 26,899.64 | 1,018.67 | 58,583.12 |
| 2010 | Water | 3.87 | 10.87 | 728.49 | 8.95 | 0.51 | 752.69 |
| | Grassland | 9.4 | 14,949.99 | 15,298.44 | 82,730.62 | 4,937.69 | 117,926.1 |
| | Built-up | 1.88 | 267.3 | 88.79 | 944.75 | 178.97 | 1,481.69 |
| | Total | 575.73 | 31,282.72 | 35,326.39 | 112,509.74 | 6,158.48 | 185,853.1 |

Table 5: Accuracy assessment results for 2000, 2010 and 2020

| | Year | | | | | |
|---|---|---|---|---|---|---|
| | 2000 | | 2010 | | 2020 | |
| Land cover | Producer accuracy | User accuracy | Producer accuracy | User accuracy | Producer accuracy | User accuracy |
| Close Forest | 0.7143 | 0.7143 | 1 | 0.8571 | 1 | 1 |
| Open Forest | 0.9091 | 0.8 | 0.7778 | 0.7 | 0.7692 | 0.625 |
| Water | 1 | 1 | 1 | 1 | 1 | 1 |
| Grassland | 0.85 | 0.9444 | 0.7692 | 0.8333 | 0.76 | 0.8261 |
| Built-up | 0.8333 | 1 | 0.8333 | 1 | 0.875 | 1 |
| Overall accuracy | 0.8667 | | 0.8167 | | 0.8333 | |
| Percentage accuracy | 86.67 | | 81.67 | | 83.33 | |
| Kappa coefficient | 0.81 | | 0.7389 | | 0.7732 | |

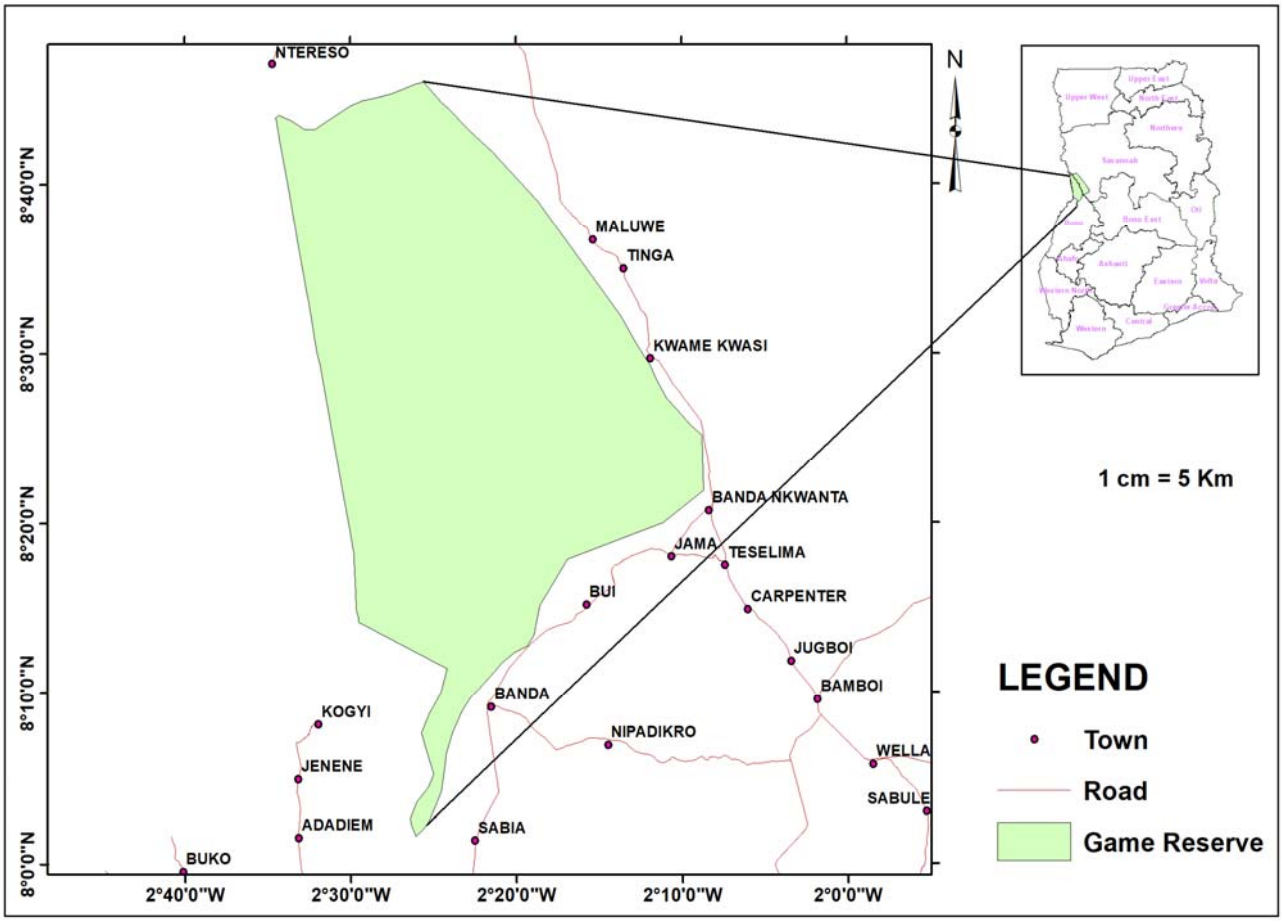


Figure 1: Map of study area

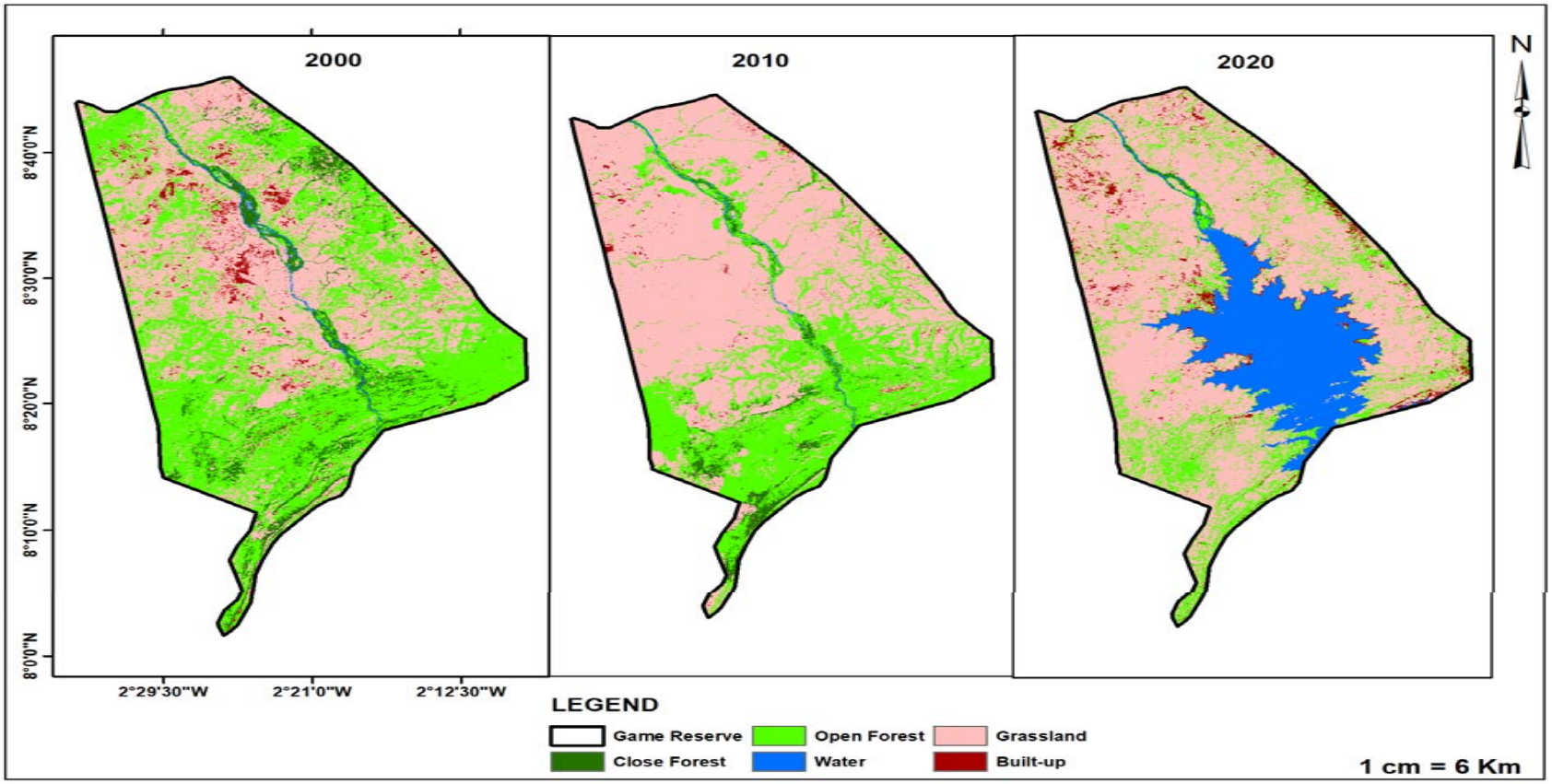


Figure 2: Land cover maps of the Bui National Park for the years 2000, 2010 and 2020.

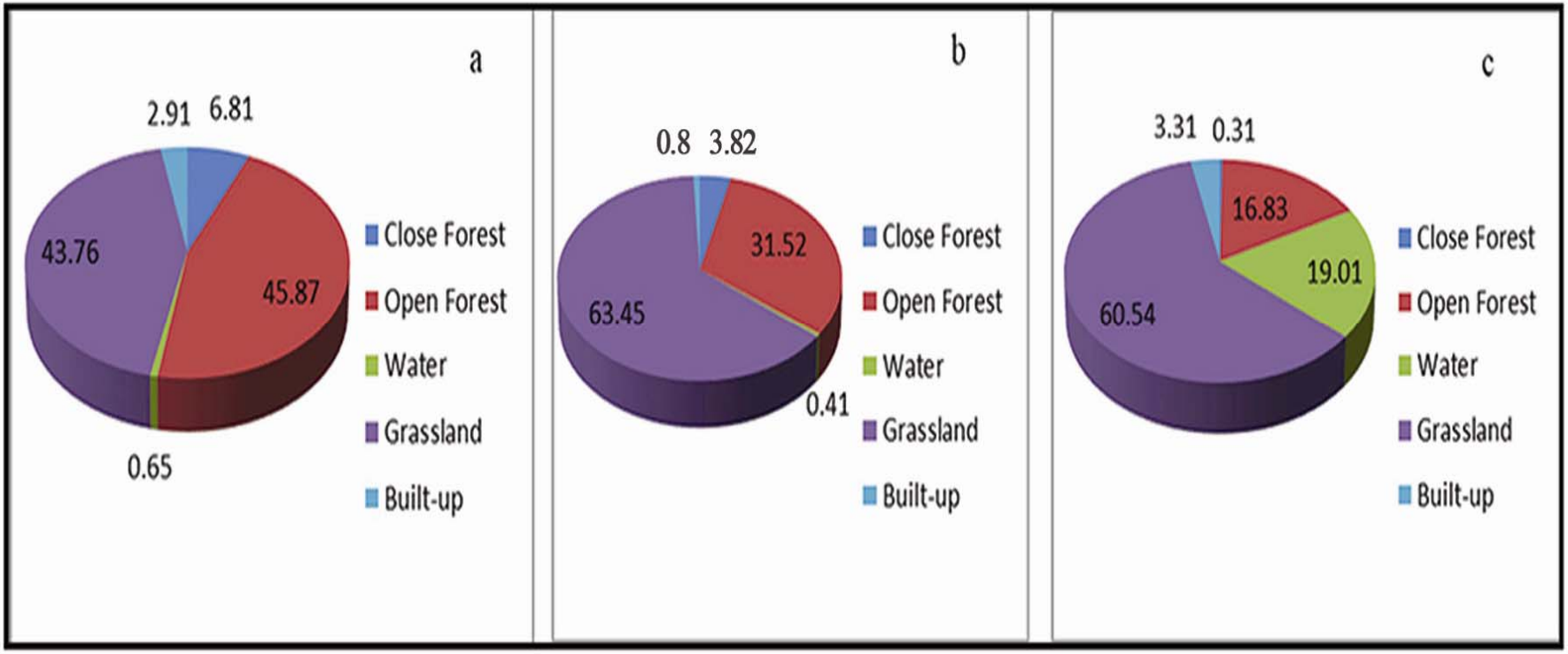


Figure 3: Percentage of area covered by each Land cover types; a) 2000, b) 2010 and c) 2020